HHS Public Access

Author manuscript

Immunol Cell Biol. Author manuscript; available in PMC 2017 May 29.

Published in final edited form as:

Immunol Cell Biol. 2017 February ; 95(2): 215–223. doi:10.1038/icb.2016.83.

Batf3 selectively determines acquisition of CD8+ dendritic cell phenotype and function

Janin Chandra[1], **Paula TY Kuo**[1], **Anne M. Hahn**[1], **Gabrielle T. Belz**[2], and **Ian H. Frazer**[1]

[1]The University of Queensland Diamantina Institute, Translational Research Institute, Woolloongabba, Queensland 4102, Australia

[2]Walter and Eliza Hall Institute of Medical Research, 1G Royal Parade, Parkville, Melbourne, Victoria, 3052, Australia; and Department of Medical Biology, University of Melbourne, Melbourne, Victoria 3010, Australia

Abstract

Batf3 is a transcription factor that impacts the development of CD103+ tissue-resident dendritic cells (DCs). However, whether Batf3 is absolutely required for the development of CD8+ DCs remains controversial. Id2 is required for CD8+ DC development. Here we show that bone marrow chimeric mice with a deletion of Id2 in the CD11c compartment lose the ability to reject a skin graft expressing a non-self protein antigen or mount a delayed hypersensitivity response. In contrast, Batf3−/− mice remained competent for skin graft rejection and delayed hypersensitivity, and retained a CD8+ DC population with markers characteristic of the CD11b+ DC lineage including CD11b, CD4 and CD172α as well as the key regulator transcription factor IRF4, but lacked IRF8 expression. CD8+ DCs in Batf3−/− mice took up and cleaved protein antigen and larger particles but were unable to phagocytose dying cells, a characteristic feature to the CD8+ DC lineage. These data clarify a requirement for CD8+ lineage DCs for inducing effectors of neo-antigen driven skin graft rejection, and improve our understanding of DC subtype commitment by demonstrating that in the absence of Batf3, CD8+ DCs can change their fate and become CD11b+ DCs.

Introduction

Professional antigen-presenting cells (APCs) including dendritic cells (DCs) in the skin and draining lymph nodes play a critical role in maintaining tolerance of the adaptive immune system to beneficial skin microbiota, and conversely in priming T cells specific to proteins

Correspondence: Ian Frazer, University of Queensland Diamantina Institute, Translational Research Institute, Woolloongabba, Queensland 4102, Australia; i.frazer@uq.edu.au, T: +61 (0)4 1373 3248; +61 (0)7 3443 6962, F: +61 (0)7 3443 7779.

Conflict of interest disclosure: The authors declare no competing financial interests.

Authorship

Contribution: J.C. performed experiments, analysed and interpreted data, performed statistical analysis and drafted the manuscript. P.TY.K. and A.M.H. performed experiments and analysed data. G.T.B. reviewed the manuscript and interpreted data. I.H.F. supervised the study, interpreted data, drafted and reviewed the manuscript. G.T.B. and I.H.F. gave final approval of the submitted version. Supplementary information is available at the ICB's website.

from viruses infecting the skin including herpes-simplex and human papillomavirus (1–4). According to our current understanding, conventional DCs (cDCs) can be categorized into two main lineages, namely CD8+ DCs and CD11b+ DCs (5), with the CD8+ DC lineage being critical in promoting immunity to viral skin infection (1). Both CD11b+ and CD8+ lineages develop from common DC precursors in the bone marrow, but their functional maturation depends on different transcription factors. Development of CD8+ DCs requires Irf8, Id2, Nfil3 and Batf3, whereas development of CD11b+ DCs depends on RelB, Notch2 and Irf4 (6). The CD8+ DC lineage is of particular interest because of their ability to take up cellular material, cross-present antigen and activate CD8+ cytotoxic T cells (1, 7–11). This lineage includes tissue migratory CD103+ DCs as well as the lymphoid tissue-resident CD8+ DCs.

Mice lacking the CD8+ DC lineage, including IRF8−/−, Batf3−/− and Id2flox/flox-CD11cCre+ mice have demonstrated the importance of these DCs in a variety of disease models (12–20). However, recent reports suggest that while Batf3 may be crucial in the development of CD103+ DCs, its requirement for the development of CD8+ lymphoid tissue resident DCs can be bypassed by other factors. For example, Flt3L-driven bone marrow cultures from Batf3−/− mice will give rise to CD8+ but not CD103+ DCs (21). Furthermore, infection with *M. tuberculosis* was shown to restore both CD8+ and lung-resident CD103+ DCs in Batf3−/− mice *via* induction of IL-12 and enabled control of the intracellular bacterium comparable to wild-type mice (22). Recently, development of CD8+ DCs in Batf3−/− mice was shown to differ between different animal housing facilities (23). Petersen and colleagues showed that a CX3CR1-Langerin-CD8+ DC subset could be found in Batf3−/− mice, which they proposed to be a non-functional precursor of mature Langerin+ CD8+ DCs (24). In a recent study, bone marrow-derived pre-CD8 DCs treated with GM-CSF did not complete their development into functional CD8+ DCs in the absence of Batf3 but instead diverted to the CD11b+ lineage through expression of CD172α (25), an observation that allows speculation about plasticity within different pre-committed DC precursors.

In the present report, we used two mouse models to determine the role of CD8+ lineage DCs in neo-antigen driven skin graft rejection and delayed type hypersensitivity (DTH) to broaden our understanding on immune responses to skin tropic viral diseases or skin targeted autoimmunity (26, 27). Here, we used Id2flox/flox-CD11cCre+ chimeric mice, which lack CD8+ lineage DCs, to show that these are required for neo-antigen driven skin graft rejection and DTH. We show further that a residual CD8+ DC population exists in Batf3−/− mice which are competent for skin graft rejection and DTH. We characterised the difference in functional capacity of the different APCs in Batf3−/− animals, and provide evidence to show that, in the absence of Batf3, lymphoid tissue-resident CD8+ DCs can divert *in vivo* to the CD11b+ DC lineage.

Results and Discussion

Induction of DTH and rejection of neo-antigen expressing skin grafts are driven by CD8+ lineage DCs, but are Batf3 independent

To investigate the importance of CD8+ lineage DCs, including CD103+ migratory and CD8+ lymphoid tissue-resident DCs, in the process of neo-antigen driven skin graft rejection, we employed two transgenic mouse models with deficits in APC function. We grafted OVA-expressing skin from K5mOVA transgenic mice onto mice chimeric for an Id2 deleted CD11c+ lineage (Id2flox/flox-CD11cCre+ chimeras), or onto mice deleted of the Batf3 transcription factor (Batf3−/− mice). Id2flox/flox-CD11cCre+ chimeras were unable to reject K5mOVA skin grafts, whereas there was no difference in skin graft rejection between Batf3−/− and control mice (Fig. 1a). To assess the OVA specific CD8+ T cell response generated in response to K5mOVA skin grafting, we restimulated lymph node cells of K5mOVA skin grafted mice with the MHC class I-restricted OVA peptide SIINFEKL, and determined the number of primed OVA-specific CD8+ T cells by IFNγ ELISPOT. Lymph node cells from K5mOVA skin grafted Id2flox/flox-CD11cCre+ chimeras showed a significantly reduced number of OVA-specific CD8+ IFNγ-secreting T cells when compared with grafted control mice, in keeping with their failure to reject K5mOVA grafts (Fig. 1b). Batf3−/− mice also had reduced numbers of OVA-specific CD8+ IFNγ-secreting T cells in lymph nodes after receipt of a K5mOVA skin graft, although graft rejection was comparable to control mice (Fig. 1b).

In a DTH model we tested the immune response to antigens delivered intradermally further. In line with the previous data, we found that Id2flox/flox-CD11cCre+ chimeras were significantly restricted in their ability to mount a DTH response (Fig. 1c), whereas Batf3−/− mice responded comparable to control mice (Fig. 1d). To investigate if cytotoxicity was affected in response to intradermally delivered antigens in the absence of CD8+ lineage DCs, we assessed the killing of SIINFEKL antigen-pulsed target cells in OVA-immunised mice. We found that similar to the limited IFNγ response, both Id2flox/flox-CD11cCre+ chimeras and Batf3−/− mice were significantly restricted in their ability to kill target cells (Fig. 1e).

Our data suggest that expression of the Id2 transcription factor in CD8+ lineage DCs is critical for CD8+ T cell priming, DTH and antigen driven graft rejection, and that also the Batf3 transcription factor is required for APCs to induce a maximal cytotoxic CD8+ T cell response. However, in the absence of Batf3, both DTH and neo-antigen driven skin graft rejection can be induced. In a previous study, minor antigen driven (H-Y) skin graft rejection was dependent on Batf3-dependent APCs (20). Differences in either the type of antigen, soluble or membrane located, or the distribution of antigen expression, on keratinocytes or on all somatic cells, might explain these differences. However, previous findings showing that a contact hypersensitivity response is Batf3-independent is consistent with the DTH data we describe here (12).

Batf3−/− mice contain a residual population of CD8+ DCs

A possible lack of CD8+ DCs in Batf3−/− mice has been proposed, with unclear experimental findings (19, 23, 24). We therefore analysed the peripheral DC compartment in Batf3−/− mice and Id2flox/flox-CD11cCre+ chimeras and observed a significant reduction, but not a complete absence, of CD8+ DCs in spleen of both these mice, when compared to control animals (Fig. 2a). However, the reduction of CD8+ DCs in Id2flox/flox-CD11cCre+ chimeras was more pronounced than in Batf3−/− mice. Additionally, we observed a significant increase of CD11b+ DCs in spleen of Batf3−/− mice, and a letter but significant reduction in Id2flox/flox-CD11cCre+ chimeras. CD103+ DCs in skin were absent in both mouse models (Fig. 2b). In lymph nodes of Batf3−/− mice, we found a significant reduction in CD8+ DCs and CD103+ DCs, and a significant increase in CD11b+ DCs (Supplementary Figure 2).

In the absence of Batf3, CD8+ DCs acquire a phenotype characteristic to the CD11b+ DC lineage

Diversion of bone marrow-derived CD8+ pre-DCs to the CD11b+ DC lineage, mediated by GM-CSF and in the absence of Batf3, has recently been described (25). We therefore examined DCs for a range of characteristic DC membrane proteins, and observed that the residual CD8+ DCs in Batf3−/− spleens expressed the surface markers that characterize the CD11b+ DC lineage. In detail, CD8+ DCs in Batf3−/− spleens expressed various and significantly higher levels of CD11b and CD172α compared to CD8+ DCs in control mice, and were partly CD4+ (Fig. 3a–c). This could be clearly observed by visual inspection of flow cytometry data where we plotted CD8 against CD11b, CD4 and CD172α on DCs (Fig. 3a), and by comparing mean fluorescent intensities (MFI) of these markers expressed on CD8+ DCs (Fig. 3b and c). In contrast, no up-regulation of CD11b was observed in the small population of CD8+ DCs in Id2flox/flox-CD11cCre+ chimeras. These data suggest that, in the absence of Batf3, peripheral CD8+ DCs in secondary lymphoid tissues divert to the CD11b+ DC lineage, and no such phenomenon can be observed in DCs lacking Id2.

Batf3−/− CD8+ DCs process antigen and take up particles but lose the capacity to phagocytose dying cells

Next, we investigated whether the residual CD8+ DC population in Batf3−/− mice could process exogenous antigen effectively. We incubated splenocytes from Batf3−/− and control mice with a self-quenching dye coupled to OVA (DQ-OVA) which fluoresces on tryptic cleavage, and analysed cleavage of the DQ-OVA in CD8+ and CD11b+ DCs (Fig. 4a). We observed that both CD8+ and CD11b+ DCs cleaved DQ-OVA, and that CD8+ DCs showed greater MFI than CD11b+ DCs (Fig. 4a). DQ-OVA processing in CD11b+ DCs was comparable in Batf3−/− and control splenocytes. Surprisingly, the residual population of CD8+ DCs in Batf3−/− mice processed more DQ-OVA than control CD8+ DCs, shown both by an increased percentage and MFI, suggesting that these residual Batf3−/− CD8+ DCs can process antigen efficiently. We further assessed phagocytic function by incubating splenocytes with dye-labelled liposomes. We found that both CD8+ DCs and CD11b+ DCs of control and Batf3−/− mice took up liposomes in comparable amounts, whereas no uptake was observed when samples were incubated on ice (Fig. 4b).

A characteristic feature of CD8+ DCs is their superior capacity to endocytose dying cells (28). We therefore determined whether the residual CD8+ DC population in Batf3−/− mice were able to take up dead cells. We injected labelled dying cells into Batf3−/− and control mice and found that endocytosis of dying cells was restricted to CD8+ DCs in control mice, while CD11b+ DCs showed no uptake of dying cells (Fig. 4c). Interestingly, the residual population of CD8+ DCs in Batf3−/− mice were largely unable to take up dying cells (Fig. 4c), demonstrating a loss of function and suggesting that these DCs do not functionally resemble the classical CD8+ DCs found in immunocompetent control mice. In support of this hypothesis, we recognized that a small fraction of the Batf3−/− CD8+ DCs that had endocytosed dying cells were CD11b negative, and no Batf3−/− CD8+ CD11b+ DCs had endocytosed cells (Fig. 4d). These data further suggest a process of DC divergence from the CD8+ to the CD11b+ DC lineage in the absence of Batf3, with loss of specific function of dead cell phagocytosis but not of antigen uptake and processing or uptake of particles in general.

In the absence of Batf3, CD8+ DCs lose expression of IRF8 but increase IRF4 expression

Given that IRF8 and IRF4 are key regulatory transcription factors that respectively determine the development of CD8+ lineage and CD11b+ lineage DCs, we characterized the expression of these factors in Batf3−/− DCs. We found that while CD11b+ DCs in Batf3−/− and control mice showed comparable expression of IRF4, and no expression of IRF8, the CD8+ DCs in Batf3−/− mice had downregulated IRF8 and instead expressed IRF4 in comparable levels to CD11b+ DCs (Fig. 4e, f). This data further supports a hypothesis of plasticity between CD8+ and CD11b+ DCs, which is driven by the presence or absence of Batf3 expression.

In conclusion, functional commitment of APC precursors to either the conventional CD8+ lineage or the CD11b+ lineage DCs had originally been held to be irreversible, with development of CD8+ lineage DCs dependent on transcription factors IRF8 and Id2, whereas the Batf3 transcription factor enabled DC survival. A recent study showed that development in the bone marrow of CD8+ lineage DCs requires auto-activation of IRF8, and that Batf3 was required to maintain IRF8 activation (25) and that, in the absence of Batf3, pre-CD8+ DCs lost IRF8 expression and diverted to the CD11b+ DC lineage. We show here that this process applies not only to pre-DCs in the bone marrow, but also to mature CD8+ DCs in secondary lymphoid tissues. We show further that phenotypically mature CD8+ lineage DCs develop and survive in the absence of Batf3, and that these DCs can contribute to neo-antigen driven skin graft rejection and to development of delayed type hypersensitivity. As both antigen-specific IFNy release and CD8+ T cell cytotoxic functions are significantly reduced in the absence of Batf3, the mechanisms by which DCs lacking Batf3 induce these reactions is unclear. Batf3−/− CD8+ lineage DCs express surface markers CD11b, CD172α and CD4, and key regulator transcription factor IRF4, all characteristic of CD11b+ lineage DCs, but lack expression of IRF8, characteristic of the CD8+ lineage , and fail to endocytose dying cells. Further studies are required to investigate the stability of these characteristics, and whether they can be further altered in the periphery in response to inflammation, which would have implications for our understanding of the function of particular DC subsets in health and disease.

Methods

Mice and chimeras

C57BL/6 mice and C57BL/6-SJL were obtained from the Animal Resources Centre (Perth, Australia). K5mOVA mice were obtained from H. Azukizawa (Osaka, Japan) (27) and bred in house. OT-I mice obtained from F. Cabone (Melbourne, Australia) and were bred in house with NzegGFP mice (29). Id2flox/flox mice were kindly provided from Gabrielle Belz (Melbourne, Australia) (19) and bred in house with CD11cCre+ mice to obtain Id2flox/flox-CD11cCre+ and Id2flox/+-CD11cCre+ mice. CD11cCre+ and Batf3−/− mice were purchased from Jacksons Laboratories and bred in house (13). Control mice for Batf3−/− were used as Batf3+/− or C57BL/6 intermittently. Bone-marrow chimeric mice were generated by transfer of either bone-marrow cells or embryonic liver cells. In detail, C57BL/6 or C57BL/6-SJL mice (CD45.2 or CD45.1) received a split dose of 2× 5.5Gy and were subsequently injected intravenously with either 2×10^6 embryonic liver cells of E14 foetuses or 5×10^6 bone-marrow cells flushed from femur and tibia that had been genotyped as Id2flox/flox-CD11cCre+ or Id2flox/+-CD11cCre+ (control). Mice were treated with 10 mg/ml neomycin (Sigma) in drinking water for 2 weeks to prevent bacterial infection. Bone-marrow chimeric mice were allowed 6 weeks reconstitution before entering further experiments. Effective reconstitution and significant reduction of CD8+ and CD103+ DCs in Id2flox/flox-CD11cCre+ chimeras was confirmed by flow cytometry (Supplementary Fig. 1). All mice were kept under specific pathogen-free conditions at the Biological Research Facilities of Translational Research Institute and Otto Hirschfield Facility of the University of Queensland. All animal procedures and experiments were performed in compliance with the ethical guidelines of the National Health and Medical Research Council of Australia, with approval from the IMVS Animal Ethics Committee and the University of Queensland Animal Ethics Committee (#367-13).

Skin grafting

Ear skin was transplanted onto recipient flanks as described previously(30). Briefly, donor ear skin was split into dorsal and ventral surfaces (~$1cm^2$) and placed onto the thoracic flank region of anesthetized recipients. Grafts were covered with antibiotic-permeated gauze (Bactigras, Smith and Nephew, London, UK) and bandaged with micropore tape and Flex-wrap (Lyppard, Queensland, Australia). Bandages were removed 7 days later and grafts were monitored for 7 to 8 weeks. Photographs including a ruler were taken weekly and grafts were analysed by measurement using Fiji Imaging software. Graft rejection was defined as loss of distinct border, signs of ulceration and necrosis.

DTH

Mice were immunized intradermally to the flank with 100 μg OVA (Sigma) and 20 μg QuilA in a volume of 200 μl. Seven days later, mice were challenged with 10 μg OVA delivered intradermally to the right ear in a volume of 20 μl. Ear thickness was determined by calibre measurement before OVA challenge and 24, 48 and 72 hours after OVA challenge. PBS injection to the left ear was followed as negative control.

In vivo cytotoxicity assay

Mice were immunized intradermally to the flank with 100 μg OVA (Sigma) and 20 μg QuilA in a volume of 200 μl. Seven days later, mice received a 1:40 ratio of CFSE labelled CD45.1+ reference splenocytes and CD45.2+ SIINFEKL-pulsed target splenocytes (total number 10×10^6) by intravenous injection. Target cells were pulsed with 500ng/ml SIINFEKL for 1 hour at 37_C in medium containing 10% FCS. Spleens were harvested 18 hours after target cell transfer, prepared as single cell suspension and assessed by flow cytometry for the presence of CFSE+ CD45.1+ and CD45.2+ cells.

Cell isolations

Mice were euthanized in CO_2 and organs were removed. For DC experiments, spleens were injected with or lymph nodes (axial, inguinal) were cut into small pieces and digested with 0.5 mg/ml collagenase D (Roche, Germany) diluted in PBS 10% FCS for 30 min at 37°C. Spleens and lymph nodes were disintegrated by straining though a 70 μm cell strainer (BD Pharmingen). Splenocytes were red blood cell lysed using ACK buffer. For adoptive transfer of OT-IxNzegGFP CD8+ T cells and ELISPOT assays single cell suspensions of lymph nodes (axial, inguinal and ear-draining) and spleens were prepared by mechanically disrupting the tissue and straining though a 70 μm cell strainer. CD8+ T cells were isolated using EasySep™ Mouse CD8+ T Cell Isolation Kit (StemCell Technologies) according to the manufacturer protocol. Cell counts were performed using Countess Automated Cell Counter (Invitrogen). For cell isolations from skin, ear skin was split with forceps into dorsal and ventral sides and floated epidermis facing down in 1.2 mg/ml dispase diluted in PBS (Roche, Berlin, Germany) for 60 min at 37°C. The thin epidermal layer was stripped from dermis using forceps. Dermis and epidermis were further processed separately and cut into small pieces followed by digestion with 0.5 mg/ml of collagenase D (Roche, Germany) diluted in PBS 10% FCS for 60 min at 37°C. The remaining tissue was disrupted by straining through a 70 μm cell strainer (BD Pharmingen). Total cell isolations of two ears/ one animal was used for flow cytometry analysis.

ELISPOT

OVA-specific CD8+ T cell responses were measured using IFNγ ELISPOT. The ELISPOT protocol has been previously described. Briefly, 2×10^5 cells were plated in medium containing 10% FCS in 96 well plates (Millipore) coated with 8 μg capture antibody against IFNγ (AN18, Mabtech AB, Stockholm, Sweden). Cells were restimulated with 10 μg/ml OVA peptide SIINFEKL for 24 hours. After washing, plates were incubated with a biotinylated antibody against IFNγ (R4-6A2, Mabtech AB, Stockholm, Sweden). For detection, horseradish peroxidase-conjugated strepavidin (Sigma-Aldrich, St Louis, MO) and DAB tablets (Sigma-Aldrich, St Louis, MO) were used. Spots were counted using an automated ELISPOT reader system ELR02 (Autoimmun Diagnostika GmbH, Strassberg, Germany).

Flow cytometry

Anti-mouse monoclonal antibodies (mAbs) to CD16/32 (clone 2.4G2, no. 553142, BD Pharmingen), CD45.2 (clone 104, no. 103131, Biolegend), CD8 (clone SK1, no. 100734,

Biolegend), CD11c (clone HL3, no. 557798, BD), CD11b (clone M1/70, no. 101224, Biolegend), CD103 (clone M290, no. 121405, Biolegend), MHCII (clone M5/114.15.2, no. 107628, Biolegend), CD4 (clone GK1.5, no. 553729, BD Pharmingen), CD172a (clone P84, no. 144013, Biolegend), CD45.1 (no. 562452, BD Pharmingen), IRF4 (clone 3E4, no. 11-9858, eBioscience), IRF8 (clone V3GYWCH, no. 17-9852, eBioscience) and rat IgG1 isotype (clone RTK2071, no. 400407, 400426, 400120, Biolegend) were used. For staining of myeloid cells, cells were incubated with mAbs to CD16/32 and live/dead cell fluorescent reactive dye (Invitrogen Molecular Probes, USA) for 20 min at 4_C to block unspecific staining and exclude dead cells. All mAbs were incubated for 30 min at 4_C at predetermined optimal concentrations. For intracellular staining of IRF4 and IRF8, cells were fixed and permeabilized using the FoxP3 intracellular staining kit according to manufacturer's instructions (eBioscience). Cells were acquired on a BD LSR Fortessa X20 flow cytometer and analysed using Kaluza software (Beckman Coulter).

Antigen processing

Splenic single cell suspensions were incubated for 3 hour at 37_C with 1 μg/ml DQ-OVA (Molecular Probes, Australia) in complete media, and subsequently antibody stained for flow cytometry.

Liposome uptake

Liposomes (Control liposomes PBS from Clodronate Liposomes, Netherlands) were labelled with a 1:100 dilution of 25 mg/ml DiI dye (Molecular Probes) for 30 min on ice. Splenic single cell suspensions were incubated for 90 min at 37_C or on ice with DiI-labelled liposomes in complete media at a dilution of 1:50, and subsequently stained for flow cytometry.

Endocytosis assay

Single cell suspensions of C57BL/6 spleens and thymi were labelled with 5 μM CellTrace™ Violet (Life Technologies) for 20 minutes in PBS at 37°C. Cells were washed and UV irradiated for 30 min. Death of cells was confirmed using trypan blue. 25×10^6 dying cells were injected intravenously into recipients. 3 hours later, recipients were euthanized, spleens were taken and analysed by flow cytometry for uptake of dying cells by DC subsets.

Statistics

Statistical analysis were performed with GraphPad Prism version 5.03 for Windows (GraphPad Software, San Diego, CA). Experimental groups were compared by unpaired two-tailed t-test. Differences are considered significant if $P<0.05$.

Supplementary Material

Refer to Web version on PubMed Central for supplementary material.

Acknowledgments

Funding: This work was supported by grants of NIH (IF), National Health and Medical Research Council Queensland (IF), ACRF (IF) and the postdoctoral research fellowship of University of Queensland (IF and JH).

We thank the staff of the Biological Research Facility at the Translational Research Institute for excellent technical assistance and animal care. We further thank Lynn Tolley for technical assistance in grafting experiments. This work was supported by grants of NIH, National Health and Medical Research Council Queensland, ACRF and the postdoctoral research fellowship of University of Queensland (IF and JH).

References

1. Bedoui S, Whitney PG, Waithman J, Eidsmo L, Wakim L, Caminschi I, et al. Cross-presentation of viral and self antigens by skin-derived CD103+ dendritic cells. Nat Immunol. 2009; 10(5):488–95. [PubMed: 19349986]
2. Chu CC, Ali N, Karagiannis P, Di Meglio P, Skowera A, Napolitano L, et al. Resident CD141 (BDCA3)+ dendritic cells in human skin produce IL-10 and induce regulatory T cells that suppress skin inflammation. J Exp Med. 2012; 209(5):935–45. [PubMed: 22547651]
3. Demoulin SA, Somja J, Duray A, Guenin S, Roncarati P, Delvenne PO, et al. Cervical (pre)neoplastic microenvironment promotes the emergence of tolerogenic dendritic cells via RANKL secretion. Oncoimmunology. 2015; 4(6):e1008334. [PubMed: 26155412]
4. Belz GT, Behrens GM, Smith CM, Miller JF, Jones C, Lejon K, et al. The CD8alpha(+) dendritic cell is responsible for inducing peripheral self-tolerance to tissue-associated antigens. J Exp Med. 2002; 196(8):1099–104. [PubMed: 12391021]
5. Seillet C, Belz GT. Terminal differentiation of dendritic cells. Adv Immunol. 2013; 120:185–210. [PubMed: 24070385]
6. Murphy KM. Transcriptional control of dendritic cell development. Adv Immunol. 2013; 120:239–67. [PubMed: 24070387]
7. del Rio ML, Rodriguez-Barbosa JI, Kremmer E, Forster R. CD103- and CD103+ bronchial lymph node dendritic cells are specialized in presenting and cross-presenting innocuous antigen to CD4+ and CD8+ T cells. J Immunol. 2007; 178(11):6861–6. [PubMed: 17513734]
8. den Haan JM, Lehar SM, Bevan MJ. CD8(+) but not CD8(−) dendritic cells cross-prime cytotoxic T cells in vivo. J Exp Med. 2000; 192(12):1685–96. [PubMed: 11120766]
9. Desch AN, Randolph GJ, Murphy K, Gautier EL, Kedl RM, Lahoud MH, et al. CD103+ pulmonary dendritic cells preferentially acquire and present apoptotic cell-associated antigen. J Exp Med. 2011; 208(9):1789–97. [PubMed: 21859845]
10. Allan RS, Smith CM, Belz GT, van Lint AL, Wakim LM, Heath WR, et al. Epidermal viral immunity induced by CD8alpha+ dendritic cells but not by Langerhans cells. Science. 2003; 301(5641):1925–8. [PubMed: 14512632]
11. Belz GT, Smith CM, Eichner D, Shortman K, Karupiah G, Carbone FR, et al. Cutting edge: conventional CD8 alpha+ dendritic cells are generally involved in priming CTL immunity to viruses. J Immunol. 2004; 172(4):1996–2000. [PubMed: 14764661]
12. Edelson BT, Kc W, Juang R, Kohyama M, Benoit LA, Klekotka PA, et al. Peripheral CD103+ dendritic cells form a unified subset developmentally related to CD8alpha+ conventional dendritic cells. J Exp Med. 2010; 207(4):823–36. [PubMed: 20351058]
13. Hildner K, Edelson BT, Purtha WE, Diamond M, Matsushita H, Kohyama M, et al. Batf3 deficiency reveals a critical role for CD8alpha+ dendritic cells in cytotoxic T cell immunity. Science. 2008; 322(5904):1097–100. [PubMed: 19008445]
14. Torti N, Walton SM, Murphy KM, Oxenius A. Batf3 transcription factor-dependent DC subsets in murine CMV infection: differential impact on T-cell priming and memory inflation. Eur J Immunol. 2011; 41(9):2612–8. [PubMed: 21604258]
15. Mashayekhi M, Sandau MM, Dunay IR, Frickel EM, Khan A, Goldszmid RS, et al. CD8alpha(+) dendritic cells are the critical source of interleukin-12 that controls acute infection by Toxoplasma gondii tachyzoites. Immunity. 2011; 35(2):249–59. [PubMed: 21867928]
16. Weber M, Rudolph B, Stein P, Yogev N, Bosmann M, Schild H, et al. Host-derived CD8(+) dendritic cells protect against acute graft-versus-host disease after experimental allogeneic bone marrow transplantation. Biol Blood Marrow Transplant. 2014; 20(11):1696–704. [PubMed: 25132527]
17. Engler DB, Reuter S, van Wijck Y, Urban S, Kyburz A, Maxeiner J, et al. Effective treatment of allergic airway inflammation with Helicobacter pylori immunomodulators requires BATF3-

dependent dendritic cells and IL-10. Proc Natl Acad Sci U S A. 2014; 111(32):11810–5. [PubMed: 25074917]

18. Mildner A, Jung S. Development and function of dendritic cell subsets. Immunity. 2014; 40(5): 642–56. [PubMed: 24837101]
19. Seillet C, Jackson JT, Markey KA, Brady HJ, Hill GR, Macdonald KP, et al. CD8alpha+ DCs can be induced in the absence of transcription factors Id2, Nfil3, and Batf3. Blood. 2013; 121(9):1574–83. [PubMed: 23297132]
20. Atif SM, Nelsen MK, Gibbings SL, Desch AN, Kedl RM, Gill RG, et al. Cutting Edge: Roles for Batf3-Dependent APCs in the Rejection of Minor Histocompatibility Antigen-Mismatched Grafts. J Immunol. 2015; 195(1):46–50. [PubMed: 26034174]
21. Jackson JT, Hu Y, Liu R, Masson F, D'Amico A, Carotta S, et al. Id2 expression delineates differential checkpoints in the genetic program of CD8alpha(+) and CD103(+) dendritic cell lineages. EMBO J. 2011
22. Tussiwand R, Lee WL, Murphy TL, Mashayekhi M, Kc W, Albring JC, et al. Compensatory dendritic cell development mediated by BATF-IRF interactions. Nature. 2012; 490(7421):502–7. [PubMed: 22992524]
23. Mott KR, Maazi H, Allen SJ, Zandian M, Matundan H, Ghiasi YN, et al. Batf3 deficiency is not critical for the generation of CD8alpha(+) dendritic cells. Immunobiology. 2015; 220(4):518–24. [PubMed: 25468565]
24. Petersen TR, Knight DA, Tang CW, Osmond TL, Hermans IF. Batf3-independent langerin-CX3CR1-CD8alpha+ splenic DCs represent a precursor for classical cross-presenting CD8alpha+ DCs. J Leukoc Biol. 2014; 96(6):1001–10. [PubMed: 25170118]
25. Grajales-Reyes GE, Iwata A, Albring J, Wu X, Tussiwand R, Kc W, et al. Batf3 maintains autoactivation of Irf8 for commitment of a CD8alpha(+) conventional DC clonogenic progenitor. Nat Immunol. 2015; 16(7):708–17. [PubMed: 26054719]
26. Mattarollo SR, Yong M, Tan L, Frazer IH, Leggatt GR. Secretion of IFN-gamma but not IL-17 by CD1d-restricted NKT cells enhances rejection of skin grafts expressing epithelial cell-derived antigen. J Immunol. 2010; 184(10):5663–9. [PubMed: 20410490]
27. Azukizawa H, Dohler A, Kanazawa N, Nayak A, Lipp M, Malissen B, et al. Steady state migratory RelB+ langerin+ dermal dendritic cells mediate peripheral induction of antigen-specific CD4+ CD25+ Foxp3+ regulatory T cells. Eur J Immunol. 2011; 41(5):1420–34. [PubMed: 21469094]
28. Iyoda T, Shimoyama S, Liu K, Omatsu Y, Akiyama Y, Maeda Y, et al. The CD8+ dendritic cell subset selectively endocytoses dying cells in culture and in vivo. J Exp Med. 2002; 195(10):1289–302. [PubMed: 12021309]
29. Waddell A, Ahrens R, Steinbrecher K, Donovan B, Rothenberg ME, Munitz A, et al. Colonic eosinophilic inflammation in experimental colitis is mediated by Ly6C(high) CCR2(+) inflammatory monocyte/macrophage-derived CCL11. J Immunol. 2011; 186(10):5993–6003. [PubMed: 21498668]
30. Mittal D, Kassianos AJ, Tran LS, Bergot AS, Gosmann C, Hofmann J, et al. Indoleamine 2,3-Dioxygenase Activity Contributes to Local Immune Suppression in the Skin Expressing Human Papillomavirus Oncoprotein E7. J Invest Dermatol. 2013

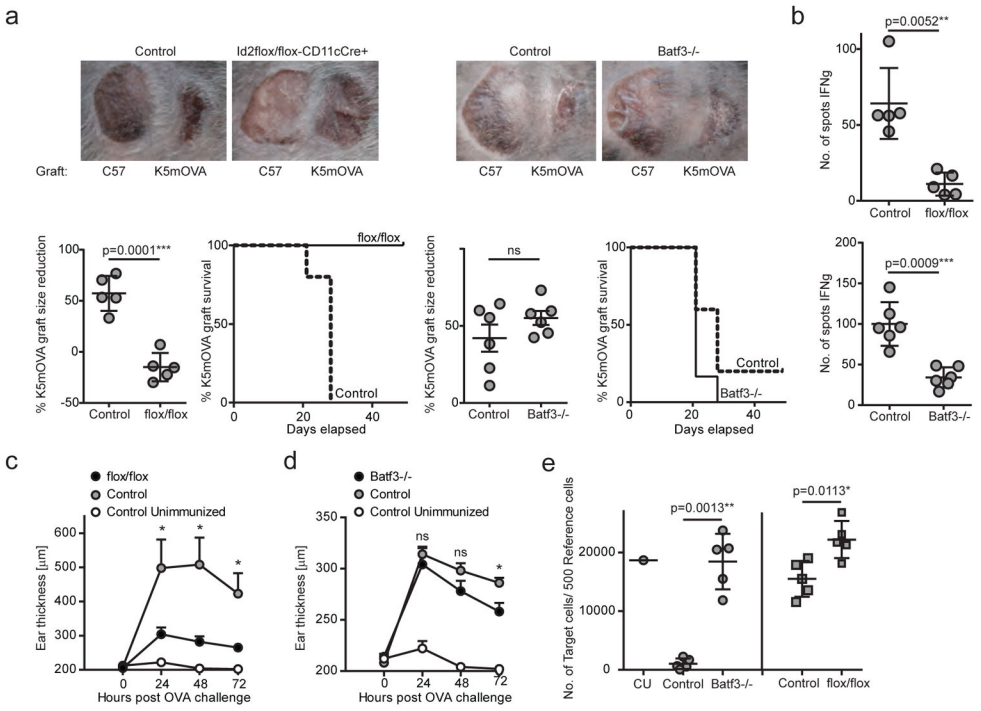

Figure 1. Batf3-independent but not Id2-independent CD8+ DCs contribute to neo-antigen driven skin graft rejection and DTH

(a) Ear skin of C57BL/6 (left) and K5mOVA (right) mice was grafted onto Id2flox/flox-CD11cCre+ (flox/flox) and control chimeras or Batf3−/− and control mice. Grafts were assessed and measured weekly for 7 to 8 weeks. Shown are representative photographs of one mouse per group. Size of grafts was depicted using imaging software. Each point represents one animal with indication of mean +/− SD of whole group (n=5–6). Graft survival curves depict loss of grafts defined as necrosis and ulceration. **(b)** At termination of the grafting assessment, lymph node cells were restimulated with SIINFEKL and IFN**γ**-producing T cells were counted by ELISPOT. Each point represents one animal with indication of mean +/− SD of whole group (n=5–6). **(c–d)** Id2flox/flox-CD11cCre+ (flox/flox) and control chimeras (c) or Batf3−/− and control mice (d) were immunized intradermally with OVA and QuilA. Seven days later, mice were challenged with OVA delivered to ear skin. Ear thickness was measured before and up to 72 hours post OVA injection. Each point represents means +/− SEM of whole group (n=10 of two independent pooled experiments for c, n=5 of one independent experiment for d) at 24, 48 and 72 hours post OVA challenge. **(e)** Id2flox/flox-CD11cCre+ (flox/flox) and control chimeras or Batf3−/− and control mice were immunized intradermally with OVA and QuilA. Seven days later, mice received a 1:40 ratio of CFSE labelled naked reference and SIINFEKL-pulsed target cells delivered intravenously. Spleens were analysed for killing of target cells 18 hours after transfer by flow cytometry. The graph indicates the number of target cells per 500 reference cells. CU: Control Unimmunized. Each point represents one animal with indication of mean +/− SD of whole group (n=5). Shown is one of two independent experiments. For statistics, transgenic mice were compared with controls. *, $p<0.05$; **, $p<0.01$; ***, $p<0.001$; ****, $p<0.0001$ (unpaired two-tailed t-test).

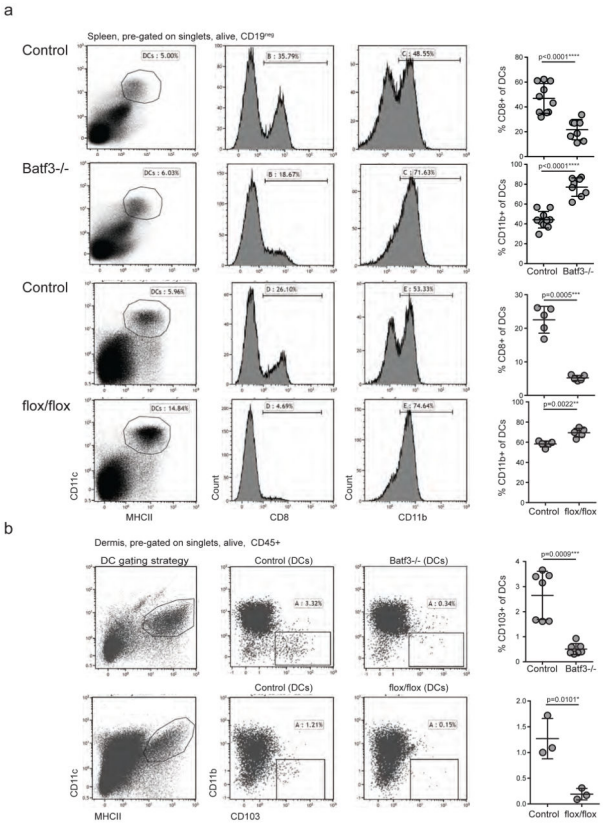

Figure 2. Batf3−/− mice contain a residual population of CD8+ DCs and increased numbers of CD11b+ DCs

(a) Splenocytes of Batf3−/−, Id2flox/flox-CD11cCre+ chimeras and control mice were analysed by flow cytometry. CD11c+ MHCII+ DCs (pre-gated on live singlets, CD19neg, TCRβneg) were assessed for expression of CD8 and CD11b. Each row of flow cytometry plots stems from one representative mouse per group. Each point in graph represents one animal with indication of mean +/− SD of whole group. (n=5 to 10, pooled from up to 3 independent experiments). **(b)** Ear skin of Batf3−/−, Id2flox/flox-CD11cCre+ chimeras and control mice was separated into dermis and epidermis. Live singlets, CD45+ cells were assessed for a population of MHCII+ CD11c+ DCs that was further gated onto CD103+ DCs by flow cytometry. In the graph, each point represents one animal with indication of mean +/− SD of whole group. For Batf3−/− mice shown are data pooled from 2 independent experiments (n=7). For Id2flox/flox-CD11cCre+ chimeras shown is one representative from 2 independent experiments, n=3). For statistics, transgenic mice were compared with controls. *, p<0.05; **, p<0.01; ***, p<0.001; ****, p<0.0001 (unpaired two-tailed t-test).

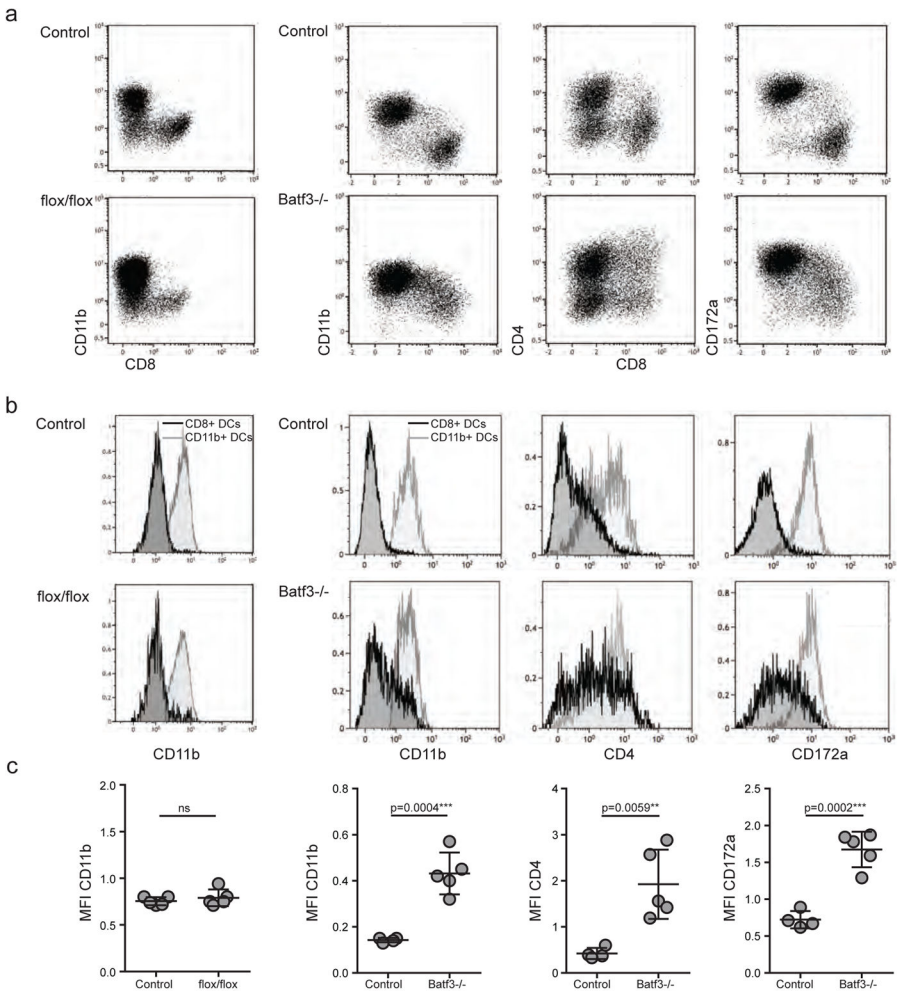

Figure 3. Batf3-independent but not Id2-independent CD8+ DCs express CD11b, CD4 and CD172α

(a) DCs in spleens of Id2flox/flox-CD11cCre+ chimeras (flox/flox) and controls or Batf3−/− and controls were gated as live singlets, CD19neg, TCRβneg, MHCII+ and CD11c+ as depicted in Figure 2. From these cells, expression of CD8 was plotted against CD11b, CD4 and CD172α. Shown are flow cytometry plots for one representative mouse per group. **(b)** DCs gated as depicted in C were further gated onto CD8+ DCs and CD11b+ DCs according to the gating strategy used in Supplementary Figure 1. Overlay histograms represent expression of CD11b, CD4 and CD172α of CD8+ DCs (black line) and CD11b+ DCs (grey line). **(c)** The median fluorescent intensity of CD11b, CD4 and CD172α of CD8+ DCs in Id2flox/flox-CD11cCre+ (flox/flox), Batf3−/− and control mice from data shown in C and D was compared. Each point represents one animal with indication of mean +/− SD of whole group (n= 4 to 5, pooled from 2 of 4 independent experiments). For statistics, transgenic mice were compared with controls. *, P<0.05; **, P<0.01; ***, P<0.001; ****, P<0.0001 (unpaired two-tailed t-test).

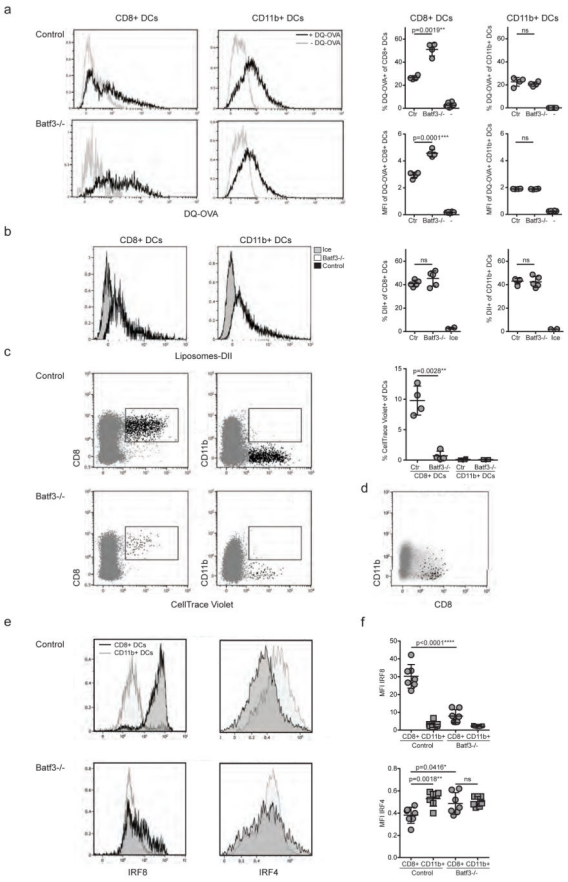

Figure 4. IRF4-expressing CD8+ DCs in Batf3−/− mice are able to process antigen but lose capacity to take up dying cells

(a) Splenocytes of Batf3−/− and control mice were incubated with DQ-OVA for 3 hours and subsequently analysed by flow cytometry for DQ-OVA processing. CD8+ and CD11b+ dendritic cell subsets were gated as shown in Figure 2. Shown are representative histograms of green fluorescence (DQ-OVA) of treated versus untreated CD8+ and CD11b+ DCs in Batf3−/− and control splenocytes. The percentage and MFI of DQ-OVA+ CD8+ or CD11b+ DCs as well as of untreated samples (−) was compared. Each point represents a sample of one animal with indication of mean +/− SD of whole group (n=4). Shown is one of two independent experiments. **(b)** Splenocytes of Batf3−/− and control mice were incubated with DiI-labelled liposomes for 90 min and subsequently analysed by flow cytometry for liposome uptake. Shown are representative histograms of red fluorescence (DiI+) of CD8+ and CD11b+ DCs in Batf3−/− and control splenocytes incubated at 37°C or on ice. The percentage of DiI+ cells of CD8+ or CD11b+ DCs was compared. Each point represents a sample of one animal with indication of mean+/− SD of the whole group (n=5). **(c–d)** CellTrace Violet labelled, UV irradiated dying cells were injected into Batf3−/− and control mice. 3 hours later, splenic CD11b+ and CD8+ DCs were analysed for endocytosis of dying cells. **(c)** Shown are flow cytometry plots that were pre-gated on DCs as shown in Supplementary Figure 1, then CellTrace Violet was plotted against CD8+ and CD11b+. CellTrace Violet+ cells depict DCs that endocytosed dying cells. In the graph, shown are percentages of CellTrace Violet+ cells of CD8+ and CD11b+ DCs. Each point represents

one animal with indication of mean +/− SD of the whole group (representative of three independent experiments, n=4). **(d)** Whole DCs (grey) and CellTrace Violet+ CD8+ DCs (black) of one representative Batf3−/− mouse from (c) was plotted against CD11b to indicate that CellTrace Violet+ CD8+ DCs are CD11b-. **(e–f)** Splenocytes of Batf3−/− and control mice were surface stained for DC markers and intracellular stained for IRF4 and IRF8. Splenocytes were pre-gated on live singlets, CD19neg, TCRβneg, MHCII+ and CD11c+, CD8+ or CD11b+ (as depicted in Figure 2). **(e)** Shown are representative histograms of IRF8 and IRF4 expression of CD8+ (black line) and CD11b+ DCs (grey line) of one mouse per group. **(f)** Mean fluorescent intensities of IRF4 and IRF8 in CD8+ and CD11b+ DCs are depicted. Each point represents one animal with indication of mean +/− SD of whole group. Shown is data of two pooled independent experiments (n=7). For statistics, transgenic mice were compared with controls. *, P<0.05; **, P<0.01; ***, P<0.001; ****, P<0.0001 (unpaired two-tailed t-test).